

# INVESTIGATION OF THE MECHANISMS OF ${}^6\text{Li}$ -INDUCED REACTIONS AT INTERMEDIATE ENERGIES

C.M. Castaneda, H.A. Smith, Jr., P.P. Singh, J. Jastrzebski†, H.J. Karwowski††,  
and A.K. Gaigalas\*

The dissociation of  ${}^6\text{Li}$  in the field of a target nucleus has been investigated in many kinematically complete <sup>1),2)</sup> and incomplete<sup>3)</sup> experiments in an effort to ascertain the reaction mechanisms present. Processes such as (a) sequential breakup of  ${}^6\text{Li}$  from its 2.18-MeV  $3^+$  state into  $\alpha+d$ , (b) non-sequential breakup into  $\alpha+d$ , (c) breakup of  ${}^5\text{Li}$  into  $\alpha+p$ , following neutron transfer, and (d) breakup of  ${}^8\text{Be}$  into  $\alpha+\alpha$  following a deuteron pickup have been found to play roles of varying importance depending upon the  ${}^6\text{Li}$  bombarding energy<sup>1)</sup>. From the variation with  ${}^6\text{Li}$  energy of the inclusive production cross sections of certain isotopes observed through in-beam  $\gamma$ -ray studies following  ${}^6\text{Li}$  bombardment of  ${}^{197}\text{Au}$ <sup>4)</sup> and  ${}^{104-106}\text{Pd}$ <sup>5)</sup>, it appeared as if some of the isotopes were produced by a mechanism whereby one of the projectile fragments interacted with the target in the manner of a (fragment, xn) reaction subsequent to the  $\alpha+d$  dissociation of the  ${}^6\text{Li}$ . We have performed charged-particle- $\gamma$ -ray coincidence measurements the results of which support the existence of such a mechanism.

The measurements were made using 75-MeV and 100-MeV  ${}^6\text{Li}^{++}$  IUCF beams and consisted of (a) observation of the charged-particle energy spectra and angular distributions over an angular range of  $10^\circ$  to  $60^\circ$  in 2 to 5-degree steps and

(b) spectra of  $\gamma$ -rays in prompt coincidence with selected charged particles. The targets chosen were  ${}^{56}\text{Fe}$  and  ${}^{197}\text{Au}$  for which the inclusive  $\gamma$ -ray spectra had been obtained in this laboratory <sup>6),7)</sup> and elsewhere<sup>4)</sup>. The charged particles were detected by means of a three-element  $\Delta E$ -E telescope, employing a 150  $\mu\text{m}$   $\Delta E$  and a 5.0 mm and 3.0 mm E silicon surface-barrier detectors. The  $\gamma$  rays were observed with a 30-cm<sup>3</sup> coaxial Ge(Li) detector with the detector axis oriented in the reaction plane and at  $90^\circ$  with respect to the beam direction. Particle- $\gamma$ -ray coincidence events were defined as prompt coincidences between the  $\Delta E$  and  $\gamma$ -ray detector signals, with a time resolution of approximately 10 ns. Both the angular distribution and particle- $\gamma$  coincidence data were recorded event-by-event on magnetic tape, and digital gates on quantities of interest were imposed during playback of the event tapes.

The discussion presented below emphasizes our particle- $\gamma$  coincidence results from the bombardment of  ${}^{197}\text{Au}$ . In this case, charged-particle emission channels in the total  ${}^6\text{Li}$  fusion-emission reaction are not significant because of the large Coulomb barrier. Our coincidence data with the  ${}^{56}\text{Fe}$  target also show very definite features similar to those

presented for the  $^{197}\text{Au}$  target. However, unambiguous interpretation of the  $^{56}\text{Fe}$  results is more difficult because of the stronger presence of the evaporation and pre-equilibrium emission of charged particles and the particle- $\gamma$  coincidence events they generate.

Typical  $\alpha$ -particle, deuteron,  $^3\text{He}$ , and triton energy spectra are characterized by a broad (10-15 MeV FWHM) peak centered at an energy corresponding to the beam velocity (see Figure 1). These "beam-velocity" particle groups exhibit angular distributions which appear to peak at an angle slightly forward of the  $^6\text{Li}$ -target Rutherford

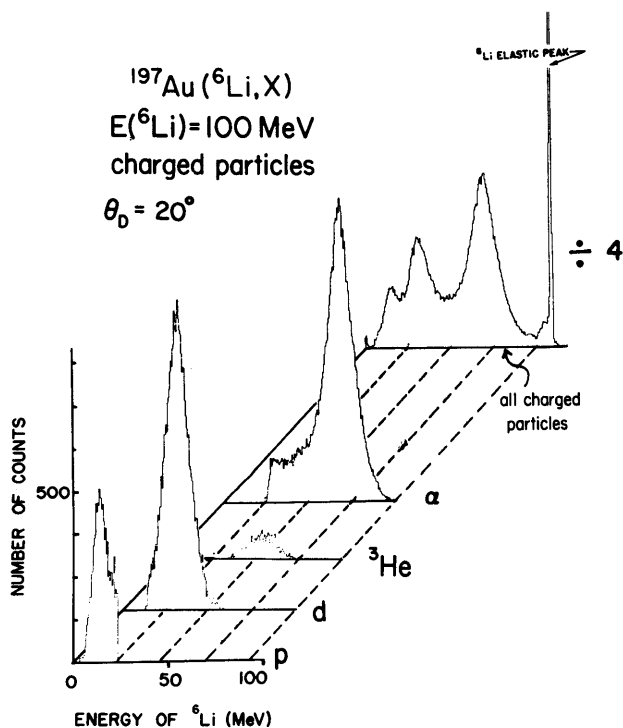


Figure 1. Typical selected charged particle spectra from the bombardment of  $^{197}\text{Au}$  with 100 MeV  $^6\text{Li}$ , the particles being observed at a lab angle of  $20^\circ$ .

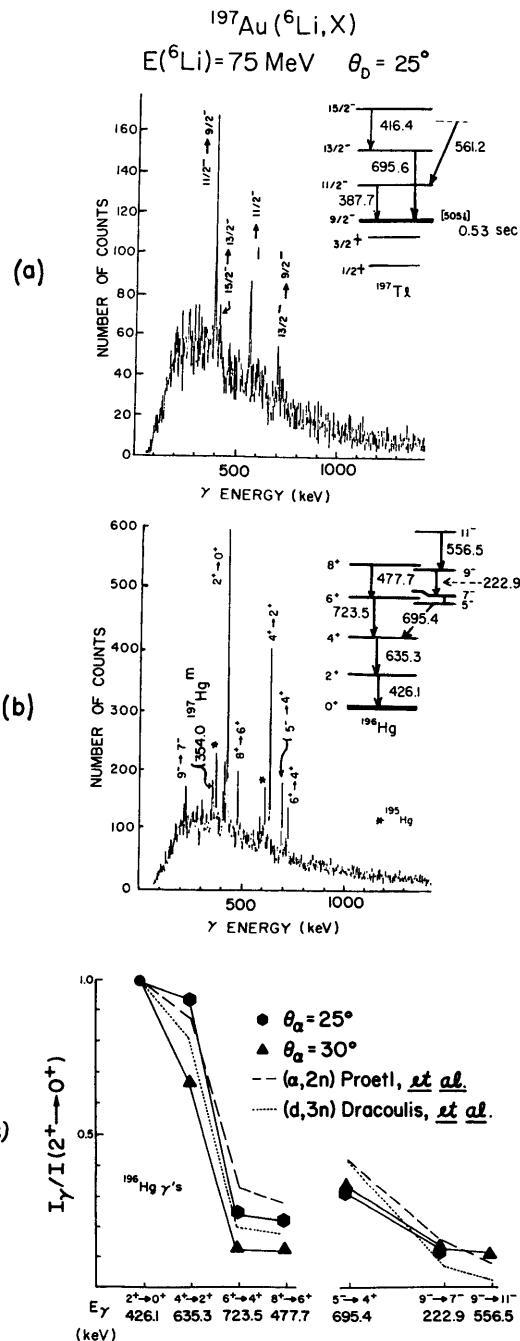


Figure 2. Spectra of  $\gamma$  rays in prompt coincidence with (a) beam-velocity deuterons and (b) beam-velocity  $\alpha$ -particles, detected at  $25^\circ$  (lab) from a 75-MeV  $^6\text{Li}$  bombardment of  $^{197}\text{Au}$ . (c) Comparison of  $^{196}\text{Hg}$  cascade  $\gamma$ -ray intensities measured in the present work from the 75-MeV bombardment with their counterparts as measured by  $(\alpha, 2n)$  11) and  $(d, 3n)$  12).

grazing angle,  $\theta_g$ , and which fall off smoothly and quickly as the laboratory charged-particle angle increases beyond  $\theta_g$ . The grazing-angle peaking is much less apparent at 100 MeV than at 75 MeV. Integration of the 75 MeV angular distributions yields the total "beam velocity particle production" cross sections from which it appears that the relative yields of all of the beam-velocity fragments are independent of the target used. This suggests

that these yields are determined more by the properties of the projectile than of the target.

The central feature of this experiment is the measurement of the spectra of  $\gamma$  rays in coincidence with these beam-velocity charged particles. In Figures 2a and 2b are shown the  $\gamma$ -rays in prompt coincidence with the beam-velocity deuterons and  $\alpha$  particles, detected at the  ${}^6\text{Li}$ -target Rutherford

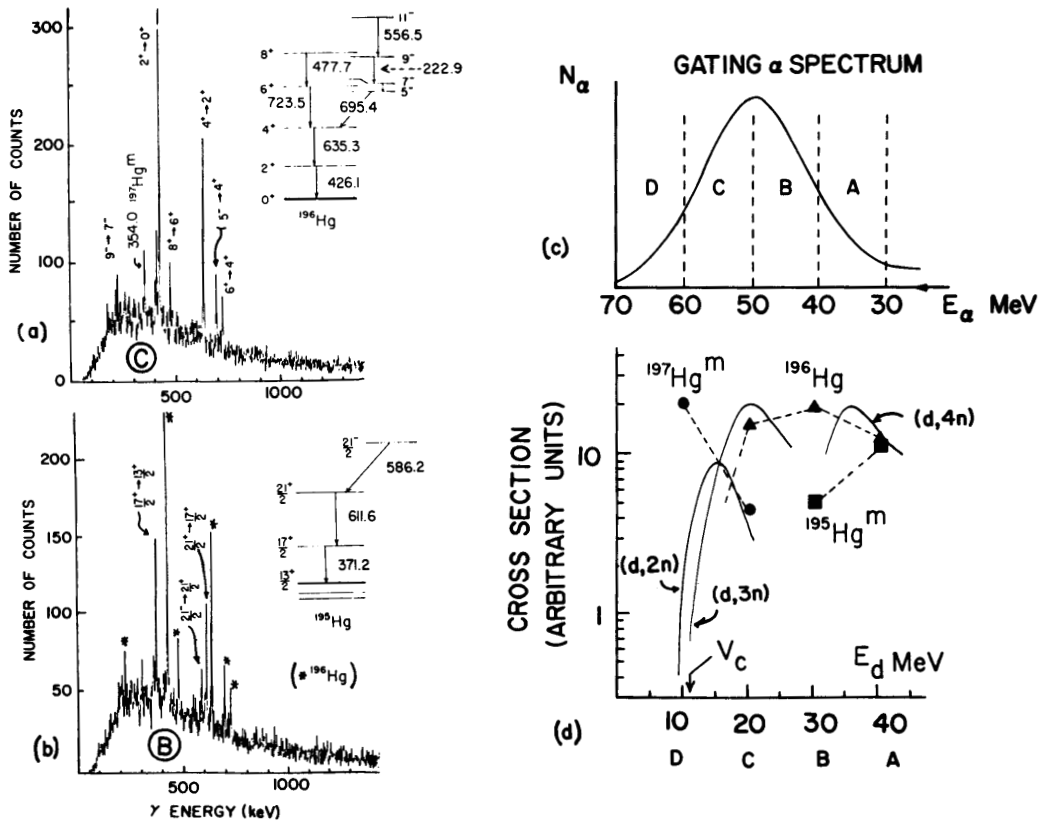


Figure 3. (a)  $\gamma$  rays in prompt coincidence with the 50-60 MeV portion of the beam velocity  $\alpha$ -particle group from the 75 MeV  ${}^6\text{Li}$  bombardment of  ${}^{197}\text{Au}$ . (b)  $\gamma$  rays in prompt coincidence with the 40-50 MeV portion of the same beam-velocity  $\alpha$ -particle group. (c) Schematic of the subdivision of the gating beam velocity  $\alpha$ -particle group for the display of the "excitation function" in Figure d. (d) Measured relative production cross section for  ${}^{195,196,197}\text{Hg}$  cascades in coincidence with specific energy groups in the beam-velocity  $\alpha$ -particle spectrum and comparison with measured  $(d,2n)$ ,  $(d,3n)$ , and  $(d,4n)$  excitation functions. The "deuteron energy" at which the data points were plotted corresponds to  $(75 - E_\alpha)$  MeV, where  $E_\alpha$  is the central energy of the gating  $\alpha$ -particle subgroup.

grazing angle ( $25^\circ$ ) for 75-MeV  ${}^6\text{Li}$  bombardment of  ${}^{197}\text{Au}$ . The prominent  $\gamma$  rays in the coincidence spectra belong to  ${}^{197}\text{Tl}$  and  ${}^{196}\text{Hg}$  respectively. The transitions which lead to their production are depicted in the energy level diagrams in the inset next to each spectrum.

Another feature of the particle- $\gamma$  coincidence data is shown in Figure 3. In Figures 3a and 3b we show spectra of  $\gamma$  rays in coincidence with selected energy "bins" of the beam-velocity  $\alpha$ -particle distribution for 75-MeV bombardment of  ${}^{197}\text{Au}$  (bins are indicated schematically in Figure 3c). To the extent that  $\gamma$  rays gated on an  $\alpha$ -particle of energy  $E_\alpha$  can be associated with the deposition of a  $(75-E_\alpha)$ -MeV deuteron in the residual system, this subdivision of the  $\alpha$ -particle gating spectrum is tantamount to the observation of a  $(d, xn)$  excitation function in the residual system. Carrying this view one step further, we show in Figure 3d the normalized relative production cross section for  ${}^{195,196,197}\text{Hg}$  isotopes as a function of this deposited energy, where this cross section is defined as the absolute cascade intensity per unit  $\alpha$ -particle flux in the energy bin in question. The energy dependence of the production cross sections is also compared with the measured  $(d, 2n)$ <sup>8)</sup>,  $(d, 3n)$ <sup>9)</sup>, and  $(d, 4n)$ <sup>10)</sup> excitation functions in Figure 3d.

We have integrated the  $\gamma$ -ray coincidence yields at fixed particle detector angle,  $\theta_D = \theta_G$ , and have assumed  $\gamma$ -ray isotropy in the laboratory. In the case of the  $\alpha$ - $\gamma$  coincidence spectrum shown in Figure 2b, the measured coincidence yield per

unit particle solid angle amounts to the production of Hg isotopes with a cross section of 70 mb/sr, as compared to the singles yield of beam-velocity  $\alpha$  particles at  $\theta_\alpha = 25^\circ$  of 661 mb/sr. (All cross sections are quoted with a 15% uncertainty, arising mainly from statistical errors and uncertainties in integrated beam charge).

The above features, namely (a) the occurrence of beam-velocity particle groups, (b) their forward-peaked angular distributions, (c) the coincidence  $\gamma$ -ray yields of specific nuclei and (d) the pattern of coincidence  $\gamma$ -ray yield with different energy bins of the gating particle can best be understood in terms of a non-sequential breakup model. Here one imagines that the incident  ${}^6\text{Li}$  breaks up into  $\alpha+d$  fragments under the influence of the target nuclear field. Subsequently one of the fragments reacts with the target nucleus. Part of the time this interaction leads to a  $(\text{fragment}, xn\gamma)$  reaction, and one then observes the  $\gamma$ -ray spectra such as described above. Considering the  $\gamma$ -ray spectrum in Figure 2b, one can infer that these  $\gamma$  rays arise from the absorption by the target of a beam-velocity deuteron, stripped from the  ${}^6\text{Li}$ , resulting in a  $(d, 3n)$  reaction. Indeed, in a 75-MeV  ${}^6\text{Li}$  bombardment, a beam-velocity deuteron fragment would carry an energy of approximately 25 MeV, and the  ${}^{197}\text{Au}(d, 3n)$  reaction cross section is observed [9] to peak at approximately 21 MeV (see Figure 3d). Our measured intensities of these coincident  ${}^{196}\text{Hg}$   $\gamma$  rays are compared with  ${}^{194}\text{Pt}(\alpha, 2n)$  intensities of Proetl, et al. [11] and the recent  ${}^{197}\text{Au}(d, 3n)$  results of Dracoulis, et al. [12] in Figure 1c. The similarity of these intensity

patterns suggests a similarity between the mechanism with which the  $^{196}\text{Hg}$   $\gamma$  rays presently observed are produced and that for the cited ( $\alpha, xn$ ) reactions, with possibly the absorbed deuteron in the present measurements bringing in somewhat less angular momentum than the ( $\alpha, 2n$ ) reaction and somewhat more than the ( $d, 3n$ ) reaction. It is interesting to note that the  $^{196}\text{Hg}$   $\gamma$  ray intensity pattern observed in coincidence with  $\alpha$  particles detected at  $\theta_\alpha = 30^\circ$  (also shown in Figure 2c) suggests that slightly lower average angular momentum is brought into the compound system by those deuteron-absorption events than by the events where the  $\alpha$  particle is detected at  $25^\circ$ . This is consistent with the fact that a larger particle scattering angle corresponds (in a classical Rutherford scattering picture) to a smaller effective impact parameter and supports the hypothesis that in such a coincidence measurement it may be possible to view ( $d, xn$ ) reaction events associated with a selectable range of angular momenta. In Figure 2a, the dominance by  $^{197}\text{Tl}$  lines in the spectrum of  $\gamma$  rays in coincidence with beam velocity deuterons would correspond to an ( $\alpha, 4n$ ) reaction in this non-sequential breakup model. The  $^{197}\text{Au}(\alpha, 4n)$  reaction is known [13] to peak at  $E_\alpha = 50$  MeV, consistent with dominance by its product in the 75-MeV  $^6\text{Li}$  bombardment.

Finally, the relative production cross sections of various isotopes of Hg as a function of the mean deuteron energies associated with bins

A, B, C, and D of the beam-velocity  $\alpha$ -particle energy distributions (Figs. 3c and 3d) seem to be generally similar to the corresponding measured ( $d, xn$ ) excitation functions. The energy dependence seen in the present measurements is not as sharp as the measured ( $d, xn$ ) results, probably due in part to the ten-MeV energy average in each datum point. However, the evident similarities of the two results do lend credence to the view that the  $\gamma$ -rays in question are produced predominantly by beam-velocity deuteron absorption. Approximately 25% of the total deuteron-induced reaction cross section is observed [8,9,10] to reside in the ( $d, xn$ ) channels for 25-MeV deuterons on  $^{197}\text{Au}$ . Therefore in the context of the non-sequential breakup model described above, the  $\alpha$ - $\gamma$  coincidence yield accounts for approximately 50% of the observed yield of beam-velocity  $\alpha$ -particles. The rest of the yield must come from other reactions of the type mentioned in the introductory comments.

A second model in terms of which some of the features mentioned above can be understood is that of a fragment transfer at the optimum Q-value, giving rise to processes such as  $^{197}\text{Au}(^6\text{Li}, \alpha)^{199}\text{Hg}^*$  and  $^{197}\text{Au}(^6\text{Li}, d)^{201}\text{Tl}^*$ . In these cases, the equality of the Z/A for the  $\alpha, d$ , and  $^6\text{Li}$  causes the optimum Q-value in a simple model [14] to be such that the maximum transfer probability is for that of an  $\alpha$  or d fragment at the beam velocity. The excited nuclei  $^{199}\text{Hg}^*$  and  $^{201}\text{Tl}^*$  so produced would subsequently decay first through

neutron evaporation and then through  $\gamma$ -ray emission, producing the particle- $\gamma$  ray spectra observed in the present measurements. If the  $\alpha$ - $\gamma$  coincidence channel were dominated by this process then our observed  $\alpha$ - $\gamma$  coincidence yield of 70 mb/sr as compared with the total beam velocity  $\alpha$  yield in singles of 661 mb/sr, would force the conclusion that only about 12% of the beam-velocity  $\alpha$  yield is due to this optimum Q-value process. Furthermore, from this mechanism one should not expect any  $\alpha$ -d coincidences, except in the unlikely event that  $^{199}\text{Hg}^*$  and  $^{201}\text{Tl}^*$  decay occasionally by emission of deuterons and  $\alpha$  particles, respectively. In a non-sequential breakup picture, however, coincidences between beam velocity deuterons and  $\alpha$  particles within a kinematic breakup cone would be plentiful. Particle-particle coincidence measurements are now being carried out at this laboratory to check this point specifically.

In summary, the observed features of the particle- $\gamma$  coincidence measurements reported here can be most readily understood in terms of the breakup of the  $^6\text{Li}$  in the target nuclear field, followed by a nuclear reaction initiated on the same nucleus by one of the projectile fragments. However, the importance of the optimum Q-value transfer process cannot be ruled out solely on the basis of the particle- $\gamma$  measurements. In any event, it is clear that a substantial fraction of the beam-velocity  $\alpha$  particles and deuterons are produced without excitation of either the target or a compound system. The particle-particle corre-

lation measurements should allow us to determine how much cross section is associated with the production of the correlated "beam-velocity" fragments; and so these measurements show the most promise for characterizing the nature of the particle- $\gamma$  channel.

\*Department of Physics, SUNY; Binghamton, N.Y. 13901.

†IUCF Visiting Scientist 1976-1977. Permanent address, INR, Swierk, Poland.

††IUCF Visiting Research Assistant 1977-1978. Permanent address: INR, Swierk, Poland.

- 1) R. Ost, K. Bethge, H. Gemmeke, L. Lassen, and D. Scholz, Z. Phys. 266, 369 (1974).
- 2) D. Scholz, H. Gemmeke, L. Lassen, R. Ost, and K. Bethge, Nucl. Phys. A288, 351 (1977).
- 3) K.O. Pfeiffer, E. Speth, and K. Bethge, Nucl. Phys. A206, 545 (1973).
- 4) J. Kropp, et al., Z. Phys. A280, 61 (1977).
- 5) C.M. Castaneda, H.A. Smith, Jr., T.E. Ward, and T.R. Nees, Phys. Rev. C 16, 1437 (1977).
- 6) J. Jastrzebski, H. Karwowski, M. Sadler, and P.P. Singh, Bull. Am. Phys. Soc. 22, 1003 (1977).
- 7) J. Jastrzebski, H. Karwowski, M. Sadler, and P.P. Singh, unpublished data, (1976).
- 8) Tu. V. Khristanov, et al., Izv. Akad. Nauk, Ser. Fiz. 36, 641 (1972), and Bull. Acad. Sci. USSR. Phys. Sec. 36, 580 (1972).
- 9) M.A. Chevarier, C.R. Acad. Sci., Ser. B270, 182 (1970).
- 10) P. Jahn, et al., Nucl. Phys. A209, 333 (1973).
- 11) D. Proetl, et al., Nucl. Phys. A231, 301 (1974).
- 12) G.D. Dracoulis, private communication (1977).
- 13) H.E. Kurz, et al., Nucl. Phys. A168, 129 (1971).
- 14) W. Von Oertzen, et al., Nucl. Phys. A207, 91 (1973).